Reduced Inflammatory Threshold Indicates Skin Barrier Defect in Transglutaminase 3 Knockout Mice

Peter Bognar[1], Ilona Nemeth[1], Balazs Mayer[1], Dora Haluszka[1], Norbert Wikonkal[1], Eszter Ostorhazi[1], Susan John[2], Mats Paulsson[2], Neil Smyth[3], Maria Pasztoi[4], Edit I. Buzas[4], Robert Szipocs[5], Attila Kolonics[5], Erzsebet Temesvari[1] and Sarolta Karpati[1]

Recently, a transglutaminase 3 knockout (TGM3/KO) mouse was generated that showed impaired hair development, but no gross defects in the epidermal barrier, although increased fragility of isolated corneocytes was demonstrated. Here we investigated the functionality of skin barrier *in vivo* by percutaneous sensitization to FITC in TGM3/KO ($n=64$) and C57BL/6 wild-type (WT) mice ($n=36$). Cutaneous inflammation was evaluated by mouse ear swelling test (MEST), histology, serum IgE levels, and by flow cytometry from draining lymph nodes. Inflammation-induced significant MEST difference ($P<0.0001$) was detected between KO and WT mice and was supported also by histopathology. A significant increase of CD4+ CD25+-activated T cells ($P<0.01$) and elevated serum IgE levels ($P<0.05$) in KO mice indicated more the development of FITC sensitization than an irritative reaction. *Propionibacter acnes*–induced intracutaneous inflammation showed no difference ($P=0.2254$) between the reactivity of WT and KO immune system. As *in vivo* tracer, FITC penetration from skin surface followed by two-photon microscopy demonstrated a more invasive percutaneous penetration in KO mice. The clinically uninvolved skin in TGM3/KO mice showed impaired barrier function and higher susceptibility to FITC sensitization indicating that TGM3 has a significant contribution to the functionally intact cutaneous barrier.

Journal of Investigative Dermatology (2014) **134,** 105–111; doi:10.1038/jid.2013.307; published online 29 August 2013

INTRODUCTION

Our knowledge on epidermal differentiation and keratinization has significantly grown within the last decade. Recent studies provide a large amount of information on proteins and enzymes of the skin barrier; however, their significance in the clinical setting is only partially understood.

The epidermal barrier has a key role in skin homeostasis and mostly environmental antigens penetrating this barrier are able to induce reactions in the skin-associated adoptive and/or innate immune system and promote irritative or allergic contact dermatitis.

[1]Department of Dermatology, Venereology and Dermato-oncology, Semmelweis University, Budapest, Hungary; [2]Center for Biochemistry, Medical Faculty, Center for Molecular Medicine and Cologne Excellence Cluster on Cellular Stress Responses in Aging-Associated Diseases, University of Cologne, Cologne, Germany; [3]Centre for Biosciences, University of Southampton, Southampton, UK; [4]Department of Genetics, Cell- and Immune Biology, Semmelweis University, Budapest, Hungary and [5]Institute for Solid State Physics and Optics, Wigner RCP, Laser Applications, Budapest, Hungary

Correspondence: Sarolta Karpati, Department of Dermatology, Venereology and Dermato-oncology, Semmelweis University, Mária Utca 41, Budapest 1085, Hungary. E-mail: skarpati@t-online.hu

Abbreviations: CH, contact hypersensitivity; DBP, dibutyl-phtalate; ET, ear thickness; KO, knockout; LN, lymph node; MEST, mouse ear swelling test; PBS, phosphate-buffered saline; SPINK5, serine protease inhibitor Kazal-type 5; TG, transglutaminase (protein); TGM, transglutaminase (gene); TGM3/KO, transglutaminase 3 knockout; WT, wild type

Received 2 May 2012; revised 24 April 2013; accepted 16 May 2013; accepted article preview online 24 July 2013; published online 29 August 2013

Transglutaminases (TG) are a group of Ca 2+-dependent enzymes, which catalyze formation of covalent isopeptide bonds and produce stabilizing cross-links between protein networks. Some of these structures contribute to an effective barrier in the skin and mucosa. TGs were first described in 1959 (Clarke *et al.*, 1959), but the exact biological function of a TG enzyme, Factor XIIIa, in the process of blood coagulation was only discovered in 1968 (Pisano *et al.*, 1968). So far, eight TGs have been identified (Hitomi *et al.*, 2001; Griffin *et al.*, 2002; Eckert *et al.*, 2005). In the outer layers of the skin and hair follicle, mainly keratinocyte-type TG (TG1) and epidermal-type TG (TG3) are expressed. Defective cross-linking of the cell envelope because of mutations in the *TGM1* gene has been found in patients suffering from lammelar ichthyosis (Huber *et al.*, 1995; Russel et al., 1995). Accordingly, TGM1 knockout mice develop an erythrodermic skin with impaired barrier function (Matsuki *et al.*, 1998). Although no *in vivo* role for TG3 has been described, it is highly expressed in the late differentiating keratinocytes, corneocytes, and the hair follicles. TG3 is also a major antigen in dermatitis herpetiformis where TG3-IgA immune complexes are deposited in the papillary dermis (Sardy *et al.*, 2002).

Recently, a transglutaminase 3 knockout (TGM3/KO) mouse was generated that showed impaired hair development, but no gross defects in the epidermal barrier (John *et al.*, 2012). Here we further investigated in these mice the functionality of the skin barrier by a generally accepted and widely used Th2

mouse model of contact hypersensitivity (CH) induced by the hapten FITC solved in aceton and dibutyl-phtalate (DBP). We found a significantly larger and more progressive cutaneous inflammation at the site of FITC re-exposition in 24 and 48 hours in KO mice when compared with the C57BL/6 wild-type (WT) animals. In the current study, we used the FITC–DBP system (Kripke *et al.*, 1990; Sato *et al.*, 1998; Imai *et al.*, 2006; Maruyama *et al.*, 2007) with some modifications and demonstrated, to our knowledge, a previously unreported functional damage of the skin barrier in mice with genetic absence of TG3.

RESULTS

TGM3/KO mice skin allows significantly stronger FITC penetration *in vivo* by two-photon microscopy

We assessed the penetration pattern of FITC (solved in dimethyl sulfoxide-distilled water) on the dorsal skin surface of earlobes in anesthetized TGM3/KO and WT mice ($n=3$ per group) *in vivo* by two-photon microscopy. The penetration pattern was different between KO and WT animals. In WT mice, FITC showed a rather faint, scattered, and blurred front of fluorescence during penetration through the epidermis, in contrast to TGM3/KO mice in which a wide, sharp, 20 μm deep band-like fluorescence-front was detectable (Figure 1a and b) at 30 minutes. Quantification data based on different representative orthogonal cuts of layers captured at 30 minutes revealed significant 4.5 ± 0.5-fold increase of FITC fluorescence in TGM3/KO skin compared with control WT skin.

By a two-photon imaging of the stained skin surface, the stratum corneum presented distinctive fluorescence patterns labeling more intensively the cornified cell envelope and some corneocytes in KO than in WT animals, indicating different penetration pattern through the barrier (Figure 1d).

TGM3 KO mice show significantly increased ear swelling in response to FITC sensitization

First, we analyzed the increase in ear thickness (ET) in each group 24 and 48 hours after FITC or vehicle re-exposure, and analyzed the data for genders separately.

The average increase in ET (ΔET) among the FITC-treated female TGM3/KO mice ($n=20$) was 18 ± 13 μm at 24 hours, and 61 ± 19 μm at 48 hours. In the group of WT female animals ($n=16$), ΔET was 11 ± 6 μm at 24 hours and 16 ± 12 μm at 48 hours, showing highly significant difference at 48 hours, compared with KO animals ($P<0.0001$, Mann–Whitney test; Figure 2a).

In the vehicle-treated female TGM3/KO group ($n=12$), the average extent of ΔET was 3 ± 4 μm at 24 hours and 17 ± 14 μm at 48 hours, whereas in the vehicle-treated WT female group ($n=9$) this value was 6 ± 3 μm at 24 hours, and 7 ± 9 μm at 48 hours, respectively, showing no significant difference (Figure 2b).

In the group of male mice, similar data were found. The average ΔET in the group of FITC-treated male TGM/KO mice ($n=18$) was 19 ± 16 μm at 24 hours and 68 ± 29 μm at 48 hours. The FITC-treated WT male animals ($n=6$) exhibited an average ΔET of 10 ± 7 μm at 24 hours and 33 ± 15 μm at 48 hours, and these data were also significantly different ($P<0.0001$, Mann–Whitney test) at the 48 hours evaluation.

Among the vehicle-treated male TGM3/KO mice ($n=14$), the average ΔET reached 2 ± 3 μm at 24 hours and 10 ± 10 μm at 48 hours. Whereas in the vehicle-treated male WT group ($n=5$), these values were 3 ± 4 μm at 24 hours and 7 ± 6 μm at 48 hours, showing no significant difference between vehicle-treated groups (data not shown).

Increased cutaneous inflammation in FITC sensitized TGM3/KO mice

In parallel with the ΔET, the skin histology from the removed ears in FITC-treated TGM3/KO and WT mice showed a dermal infiltration of lymphocytes and neutrophils around the dilated small arterioles and capillaries; however, the inflammation was more pronounced /++/ in TGM3/KO than in WT /+/ animals by semiquantitative evaluation as described in Materials and Methods. Both the TGM3/KO /++/ and WT /+/ FITC-treated animals developed epidermal hyperproliferation and spongiosis. None of the vehicle-treated animals displayed histological signs of inflammation. (Figure 2c).

By toluidine blue staining, the number of subepidermal mast cells did not differ in the FITC-treated TGM3/KO and WT mice or in the vehicle-treated groups (data not shown). The average mast cell number was >10 intensely stained mast cells per field.

Demonstration of FITC$^+$ cells in draining lymph nodes (LNs) and increased level of activated T lymphocytes in FITC-sensitized TGM3/KO animals

LN cell suspensions of FITC-treated KO and WT mice ($n=5$ per group) were studied by flow cytometry. First, we wanted to explore whether in FITC-challenged mice fluorescent cells appear in the draining LNs. We could detect slightly more FITC$^+$ cells in TGM3/KO mice than in WT ones, indicating that more FITC$^+$ non-lymphocytic cells arrive from the epidermis following FITC sensitization (data not shown).

Next, we wondered whether draining LNs from TGM3/KO animals developed increased lymphocyte activation after FITC re-exposure. As shown in Figure 3, CD4+CD25+ cells corresponding to the activated T-helper cells were highly elevated in the TGM3/KO group compared with the WT controls ($P<0.01$, Mann–Whitney test). In the case of the vehicle treatment, there was no difference between the WT and KO populations (data not shown).

Significantly elevated total serum IgE levels in FITC-treated TGM3/KO mice

In parallel with T-cell activation, a significant growth in serum IgE levels was measured in sera from FITC-treated TGM3/KO mice compared with WT mice ($n=5$ in each group).

The total serum IgE levels in FITC-treated WT mice was 868 ng ml^{-1} ± 107 (SEM), whereas the total serum IgE in FITC-treated TGM3/KO mice increased to 2,810 ng ml^{-1} ± 796 (SEM), the difference proved to be significant (($P<0.05$) $P=0.042$, Student's *t*–test; Figure 4).

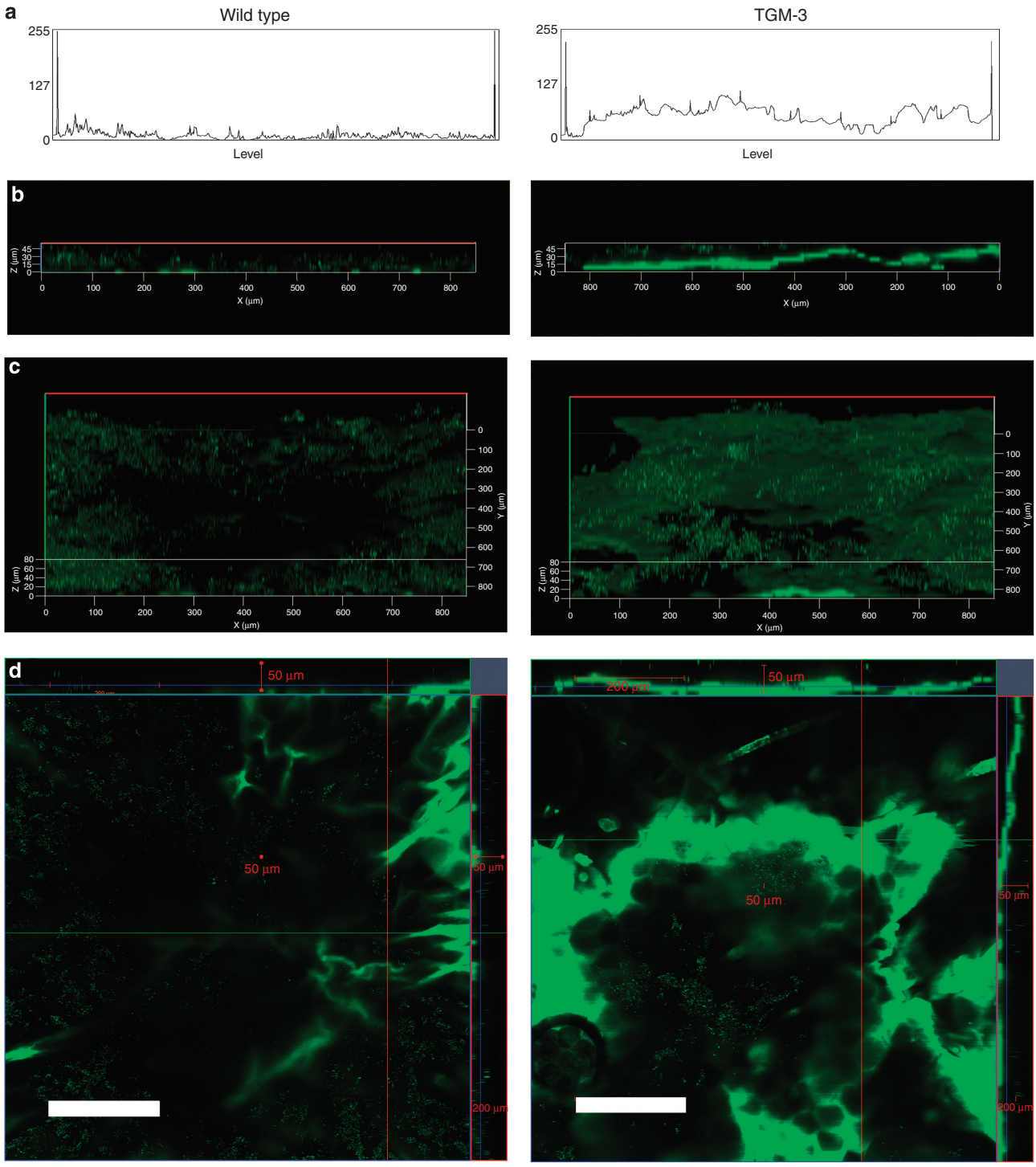

Figure 1. Penetration of FITC through stratum corneum in transglutaminase 3 knockout (TGM3/KO) and wild-type (WT) mice skin *in vivo* by two-photon microscopy. (**a**, **b**) xz-Multitracking sections composed from a stack of xy-optical sections with 8 µm distance were recorded from the skin surface ($Z = 0$ µm) down to the bottom. The representation reveals the frontal penetration profile of FITC in the TGM3/KO skin reaching an average of ~20 µm depth after 30 minutes. A more limited FITC uptake was detected in WT skin both by line analysis (**a**) and by fluorescence imaging (**b**). The line analysis demonstrates the average fluorescence intensity (on vertical axis) measured along 850 µm length of the tissue sample (horizontal axis) (**a**). (**c**, **d**) Three-dimensional images also demonstrated marked differences in FITC distribution pattern. Interconnected layers of coalescent FITC staining were found in TGM3/KO skin, whereas fine scattered FITC fluorescence was found in the WT skin (**d**, **c**). 850 µm length of the tissue sample is presented in panels **a**–**c**. On orthogonal cuts, a distinctive fluorescence pattern labeled more intensively the cornified cell envelope and some corneocytes in KO than in WT animals and indicated different penetration through the barrier. Quantification data showed significant 4.5 ± 0.5-fold increase of FITC fluorescence in TGM3/KO mice compared with WT skin (bars = 200 µm) (**d**) (study performed altogether in three mice of each group; representative data are shown).

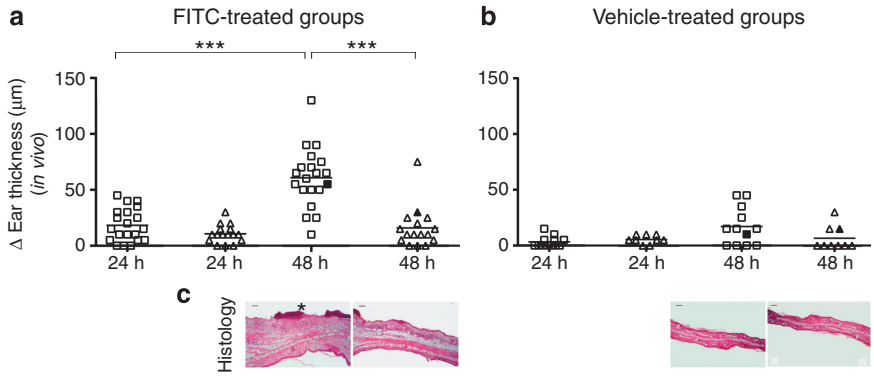

Figure 2. Significant ear thickening and histological signs of inflammation to FITC sensitization in transglutaminase 3 knockout (TGM3/KO) compared with wild-type (WT) mice. On the vertical axis, ear thickening is indicated in μm. ''□'' TGM3/KO, ''Δ'' WT mice. A significant ear thickening was detectable upon FITC treatment, between KO and WT animals at 48 hours (**a**). Although the difference was not significant, there was also more thickening in the vehicle-treated KO mice than in the vehicle WT mice (**b**). (**c**) Histology is shown for the filled symbols. TGM3/KO mice at 48 hours showed with prominent inflammation, dermal infiltration, epidermal thickening, spongiosis, and notable crust formation (marked with ''*''). WT mice developed mild-to-moderate inflammatory cell infiltration and thickened epidermis upon FITC sensitization. Vehicle-treated WT and TGM3/KO mice showed only mild edema. ***$P \leqslant 0{,}0001$, Mann–Whitney test. Bar = 40 μm.

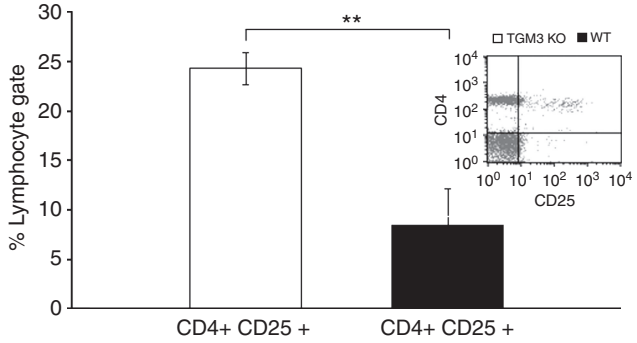

Figure 3. FACS analysis of draining lymph nodes shows an increased population of activated T-helper cells upon FITC treatment in transglutaminase 3 knockout (TGM3/KO) mice. Cells were isolated from draining lymph nodes 48 hours after re-exposure to FITC. In the inset (upper right corner), distribution of lymph node cells are shown in a FITC-treated TGM3/KO mice. Empty bars refer to TGM3/KO, black bars for wild-type (WT) mice. Data are mean ± SEM ($n = 5$). Activated T-helper cells were highly elevated in the FITC-treated TGM3/KO group when compared with the FITC-treated WT controls (**$P < 0.01$, Mann–Whitney test).

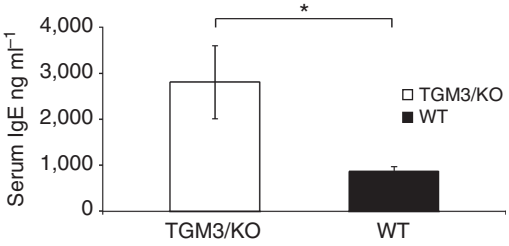

Figure 4. Significantly elevated total serum IgE levels in FITC-treated transglutaminase 3 knockout (TGM3/KO) mice. Significantly higher serum IgE levels in sera from FITC-treated TGM3/KO mice when compared with wild-type (WT) mice. Total serum IgE level in FITC-treated WT mice was 868 ng ml^{-1} ± 107 (SEM), whereas the total serum IgE in FITC-treated TGM3/KO mice increased to 2,810 ng ml^{-1} ± 796 (SEM). Empty bars refer to TGM3/KO, black bars to WT female mice. Data are mean ± SEM ($n = 5$; *$P < 0.05$, Student's *t*-test).

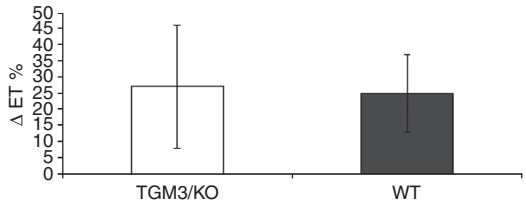

Figure 5. *Propionibacter acnes* induced mouse ear swelling test response 10^{14} colony-forming unit of *P. acnes* were injected intradermally to earlobes of transglutaminase 3 knockout (TGM3/KO) and wild-type (WT) mice. ΔEar thickness (ET) was evaluated at 24 hours. On the vertical axis, ΔET is shown in percentage (data are mean ± SEM, $n = 3$), empty column refers to TGM3/KO, black to WT mice. Ear swelling response to *P. acnes* antigen load does not show significant difference between the two groups.

Contrary, there was no significant difference in serum IgE levels between FITC-naive TGM3/KO and WT mice ($n = 5$ in each group; data not shown).

No difference in mouse ear swelling test (MEST) between TGM3/KO and WT mice after intradermal *Propionibacter acnes* injection

To investigate whether the immune system of the TGM3/KO mice are generally more reactive to antigenes compared with WT ones, we injected animals either with *P. acnes* suspension or with phosphate-buffered saline (PBS) intradermally into their two different earlobes ($n = 3$ per group). Under these circumstances, independently of the epidermal barrier, the same amount of antigen load met the immune system of KO and WT animals. We evaluated the inflammation by MEST serving the contralateral PBS-treated ear as control (Nakatsuji et *al*, 2009).

The average ET rate at 48 hours after *P. acnes* injection was related to that after PBS injcetion and the difference was 27% ± 19.3% in TGM3/KO and 25% ± 12.2% in WT mice, respectively (These values indicated no significant difference between the two groups ($P = 0.2254$, Man–Whitney test; Figure 5.). These data support the hypothesis that the higher rate of CH to FITC in TGM3/KO mice is rather a consequence

of an impaired skin barrier than an increased activity of the TGM3/KO immune system.

DISCUSSION

Defects of structural proteins like filaggrin (Sandilands *et al.*, 2007; Giwercman *et al.*, 2008), or protease inhibitors (serine protease inhibitor Kazal-type 5) and cross-linking enzymes such as TG1, have been shown to be associated with damaged cornified cell envelope formation and an enhanced percutaneous sensitization rate (reviewed by Kubo *et al.*, 2012). The role of TG3, a transglutaminase present in the cornified cell envelop and the uppermost layer of the stratum granulosum, however, remains largely unexplored in these processes. Unexpectedly, the recently developed TGM3/KO mice did not show any major barrier defect under steady-state conditions as indicated by the normal transepidermal water loss, dye penetration, and intact skin structure, although an increased fragility of the isolated corneocytes was detected (John *et al.*, 2012).

To further analyze the function and pathology of the apparently normal cutaneous barrier in animals without TG3, we chose to study the development of CH in a well-characterized FITC-induced CH mouse model. Using MEST, we detected a more severe inflammatory response in the KO animals as compared with the control group, peaking at 48 hours. Vehicle (aceton/DBP)-treated control mice showed only mild edema without significant inflammatory infiltration. KO mice showed somewhat more reaction than WT animals, but without reaching significance (Figure 2).

Although the detailed immunological analysis of FITC-induced CH generally was beyond the scope of this paper, we evaluated the CD4/CD25-activated T-cell population collected from the draining LNs, and TGM3/KO mice had significantly more activated T cells than WT cells upon FITC re-exposure, a further indicator of CH. Considering that immune responses on the background of TGM3/KO mice (C57BL/6 strain) are predominantly Th-1-biased (Takeshita *et al.*, 2004), the observed significant increase in serum IgE levels in FITC-sensitized TGM3/KO animals suggested a percutaneously induced Th2-dominated adaptive immune response (Dearman and Kimber, 2000, Larson *et al.*, 2010).

To test the non-percutaneously induced immune reactivity of TGM3/KO mice, we injected *P. acnes* intradermally to the ears of untreated mice. These bacteria are known to evoke a strong, long-lasting immune response in loco (Nakatsuji *et al.*, 2009). The similar reactivity of KO and WT animals to *P. acnes* indicated that the more severe CH provoked by FITC in TGM3/KO mice is due to an impaired skin barrier rather than a generally increased reactivity of the cutaneous immune system for other reasons.

Contrary to the normal fluorescent dye penetration observed by John *et al.* (2012), in this study we experienced an enhanced FITC entry through the cornified envelope. The different outcome can be due to the stereochemically different dyes used; Lucifer yellow has a larger molecular mass, and a vastly different water/lipid solubility as opposed to FITC, the dye that we studied. Furthermore, the penetration studies were performed previously on cadaver back skin of newborn mice, whereas in our experiments we studied 8- to 12-week-old animals and focused on the ear. It is well -known that there are structural and physiological differences between the two skin areas. Also, two-photon microscopy is considered to be a much more sensitive and precise technique than plain fluorescence microscopy, which enables us to follow real-time dye penetration.

The different FITC penetration patterns in KO and WT animals and a 4.5 ± 0.5-fold FITC fluorescence increment in TGM3/KO compared with WT skin detected by *in vivo* two-photon microscopy may serve as a further proof of damaged skin barrier function in TGM3/KO animals. The normal transepidermal water loss in these animals do not contradict our results, as the filaggrin-deficient flacky-tail mice also showed almost normal transepidermal water loss but exhibited a paracellular barrier defect and a reduced inflammatory threshold to haptens and irritants (Scharschmidt *et al.*, 2009).

All these studies verified a clinically latent barrier defect in TGM3/KO mice, which is associated with a significant susceptibility to sensitization upon percutaneous FITC challenge and indicates a reduced inflammatory threshold.

Consequently, these data suggest that the enzymatic activity of TG3 has a remarkable contribution to the epidermal barrier function.

MATERIALS AND METHODS

Mice

TGM3/KO mice (John et al, 2012) on a C57/BL6 backround (males $n = 32$, females $n = 32$) and WT animals (females $n = 25$, males $n = 11$) were studied for CH (8- to 12-week old). Further 6-6 mice were used for two-photon microscopy and *P. acnes* studies. Animals were provided food and water without restrictions, and were placed separately in cages for 24 hours before the experiment. The experiments were approved by the local ethical committee.

Contact sensitization and MEST

In all mice, the abdomen was shaved on testday (day) 0 (one day before the epicutanoeous patch installation). On day 1, an occlusive patch (Finn Chamber, diameter 18 mm (Phoenix, AZ)) saturated with 160 µl of 0.5% FITC solved in acetone/ DBP (all reagents were purchased from Sigma-Aldrich, St Louis, MO) 1:1 (v/v) mixture was fixed with adhesive tape to the prepared skin for 24 hours in knockout and WT mice. Control groups of KO and WT mice were exposed to solvent (acetone/DBP) only. The patches were removed after 24 hours (on day 2).

On day 7, the same area of the abdomen was shaved again, and on day 8, the mice were again exposed here to FITC, or to the solvent under occlusive patches.

On day 15, the baseline ET (0 hour) was measured with a digital thickness gauge just below the apex of the ear. Then the mice were challenged by 20 µl of FITC solution (0.5% FITC in acetone/DBP) on the back of both ears of the FITC-exposed animal. The control group was challenged with 20 µl of acetone/DBT. Thickening of both ears was measured at 24 and 48 hours.

Histology

Immediately after the 48 hours ET evaluation, the mice were euthanized with sodium thiopenthal (Sandoz Pharmaceutical Company, Budapest, Hungary), and both earlobes were removed.

The earlobe samples were fixed in 10% neutrally buffered formalin, and were subjected to a standard protocol of dehydration, paraffin embedding, sectioning, and staining with hematoxylin and eosin. The histological evaluation was performed blinded. We used the methods described by Hvid *et al.* (2009) with modifications. To assess the grade of inflammation, we scored the epidermal hyperplasia, spongiosis, and the presence of inflammatory cell infiltration in the dermis. A grading scale from "0" (no histopathological findings of inflammation) to "++" (severe inflammatory reaction) was used through the study.

The average number of mast cells with strong toluidine blue staining in the subepidermal area was also determined in five randomly selected microscopic fields at ×200 magnification. The used "mast cell grading scale" was as follows: "0" = 0–5 mast cells per field, "+": 6–10 mast cells per field, and "++" > 10 intensely stained mast cells per field.

Flow cytometry

Forty-eight hours after the FITC challenge on the earlobes, the draining brachial LNs (LN; 2–4 LNs per animal) were removed and single-cell suspension was prepared by gentle teasing with needles. Cells were stained with phycoerythrin-conjugated anti-mouse CD3, Peridinin Chlorophyll Protein Complex-conjugated anti-mouse CD4, and phycoerythrin-conjugated anti-mouse CD25 antibodies (all from BD Biosciences, San Jose, CA, USA). Measurments were also performed on unlabeled LN cells in order to detect the fluorescence at the wavelength of FITC in the non-lymphoid gate. The cells were studied by a Becton Dickinson FACSCalibur flow cytometer (Becton Dickinson, San Jose, CA), and the results were evaluated by the CellQuest programme version 3.1 (San Jose, CA).

Serum IgE ELISA

At the 48 hours ET evaluation, sera were obtained from both FITC-treated TGM3/KO and WT mice, and kept frozen at −20 C° until ELISA measurements.

Total serum IgE levels were measured with a commercially available mouse IgE ELISA KIT (BD Biosciences, Mouse IgE ELISA set, cat. no. 555248) together with the additional reagent set (BD Biosciences, OptEIA Reagent Set B (pH9.5 buffer) cat. no 550534) according to instructions provided by the manufacturer.

In vivo two-photon microscopy to analyze cutaneous FITC penetration in TGM3/KO and WT mice

Mice ($n = 3$ per group) were anesthetized and their earlobes were attached to microscopic slides with Vetbond 3M (3M, St Paul, MN) tissue adhesive.

FITC stock solution (5 mg ml^{-1} in dimethyl sulfoxide) was diluted 1:100 in nanopure water. A 2 µl drop was deposited onto the dorsal skin surface of the ear and was allowed to dry. Penetration of the fluorophore was measured by *in vivo* two-photon absorption fluorescence microscopy (Denk et al, 1990) and evaluated after 15, 30, and 40 minutes by a Carl Zeiss LSM 7 MP laser scanning microscope (Carl Zeiss, Jena, Germany). An optically pumped mode-locked Ti:sapphire laser (FemtoRose 100 TUN NoTouch, R&D Ultrafast Lasers, Budapest, Hungary) was used as a two-photon excitation source at a center wavelength of ~795 nm. The laser delivered ~190 fs pulses at a repetiton rate of ~76 MHz and had a Gaussian beam profile. The FITC fluorophore could be effectively excited at this wavelength (Periasamy, 2001). The average power was set by an acousto-optic device with a slight chromatic dispersion (ΔλFWHM ~40 nm), not affecting the optical pulse focusability in a spectral bandwidth of ΔλFWHM ~5 nm. The average laser power was set to ~20 mW, providing a high-fluorescence signal but no thermal or genetic damage to the sample (Antal and Szipőcs, 2012). Laser beam was focused by a ×20 water immersion objective, which also collected the fluorescent signal from the sample to a non-descanned detector. The signal passed a long pass ($\lambda > 680$ nm) dichroic filter, a corresponding laser-blocking filter, and a 500–550 nm bandpass filter before reaching the non-descanned detector.

Tissue samples ($850 \times 850 \times 80\,\mu m^3$) from anesthetized KO and WT animals were optically sliced starting from the outer surface of stratum corneum in 8 µm increments (z-stack measurements). The Three-dimensional images were captured and analyzed by the commercial ZEN software (Carl Zeiss) of the two-photon microscope.

Quantification of fluorescein imaging was performed at 30 minutes based on three independent experiments using three representative orthogonal cuts of 11 layers at 8 µm distance from each other, and were visualized as line analysis individually measured. For fluorescence intensity analysis, publicly free access UTHSCA Image Tool for Windows version 3.00 was used. Integrated fluorescence density was calculated on the full area of orthogonal cuts (Breunig *et al*, 2012, König, 2000)

P. acnes induced ear swelling

TGM3/KO and WT mice ($n = 3$ per group) were injected with 20 µl of *P. acnes* suspended in sterile PBS (1×10^{14} colony-forming unit) into the dorsal proximal site of left earlobe. As a negative control, the right earlobe was similarly treated with 20 µl PBS.

After 48 hours, the ear swelling response was measured with a digital thickness gauge.

The rate of left ear swelling to *P. acnes* was related to the PBS-induced ET and was given in percentage.

Statistical analysis

Data were analyzed by IBM SPSS Statistics 19 Software (IBM, Armonk, NY) using standard non-parametric Mann–Whitney test or Student's *t*-test.

CONFLICT OF INTEREST

The authors state no conflict of interest.

ACKNOWLEDGMENTS

We thank Judit Harsing and Daniella Kuzmanovszki (from Semmelweis University, Department of Dermatology, Venereology and Dermato-oncology, Budapest, Hungary) for their help in histological evaluation. We also thank Petra Misjak (from Department of Genetics, Cell- and Immune Biology, Semmelweis University, Budapest, Hungary) for her help in flow cytometry and data assessment. Excellent technical assistance throughout the study by Mercedesz Mazan and Dora Pinter (from Semmelweis University, Department of Dermatology, Venereology and Dermato-oncology, Budapest, Hungary) is also gratefully acknowledged. This study was supported by TÁMOP—4.2.1/B-09/1/KMR-2010-0001 and OTKA: K73296 and also by the Hungarian Development Agency (NFÜ) under contract no. TECH-09-A2-2009-0134. Neil Smyth is funded by MRC grant G0501515***, and Mats Paulsson by the Deutsche Forschungsgemeinschaft SFB 829.

REFERENCES

Ammasi Periasamy (ed) (2001) *Methods in Cellular Imaging*. Oxford University Press: New York

Antal PG, Szipőcs R (2012) Tunable, low-repetition-rate, cost-efficient femtosecond Ti:sapphire laser for nonlinear microscopy. *Appl Phys* B 107:17–22

Breunig HG, Bückle R, Kellner-Höfer M *et al.* (2012) Combined *in vivo* multiphoton and CARS imaging of healthy and disease-affected human skin. *Microsc Res Tech* 75:492–8

Clarke DD, Mycek MJ, Neidle A *et al.* (1959) The incorporation of amines into proteins. *Arch Biochem Biophys* 79:338–54

Denk W, Strickler JH, Webb WW (1990) Two-photon laser scanning fluorescence microscopy. *Science* 248:73–6

Dearman RJ, Kimber I (2000) Role of CD4(+) T helper 2-type cells in cutaneous inflammatory responses induced by fluorescein isothiocyanate. *Immunology* 101:442–51

Eckert RL, Sturniolo MT, Broome AM *et al.* (2005) Transglutaminase function in epidermis. *J Invest Dermatol* 124:481–92

Giwercman C, Lerbaek A, Bisgaard H *et al.* (2008) Classification of atopic hand eczema and the filaggrin mutations. *Contact Dermatitis* 59:257–60

Griffin M, Casadio R, Bergamini CM (2002) Transglutaminases: nature's biological glues. *Biochem J* 368(Pt 2):377–96

Hitomi K, Horio Y, Yamanishi K *et al.* (2001) Analysis of epidermal-type transglutaminase (Tgase 3) expression in mouse tissues and cell lines. *Int J Biochem Cell Biol* 33:491–8

Huber M, Rettler I, Bernasconi K *et al.* (1995) Mutations of keratinocyte transglutaminase in lamellar ichthyosis. *Science* 267:525–8

Hvid M, Jensen HK, Deleuran B *et al.* (2009) Evaluation of FITC-induced atopic dermatitis-like disease in NC/Nga mice and BALB/c mice using computer-assisted stereological toolbox, a computer-aided morphometric system. *Int Arch Allergy Immunol* 149:188–94

Imai Y, Kondo A, Iizuka H *et al.* (2006) Effects of phthalate esters on the sensitization phase of contact hypersensitivity induced by fluorescein isothiocyanate. *Clin Exp Allergy* 36:1462–8

John S, Thiebach L, Frie C *et al.* (2012) Epidermal transglutaminase (TGase 3) is required for proper hair development, but not the formation of the epidermal barrier. *PLoS One* 7:e34252

König K (2000) Multiphoton microscopy in life sciences. *J Microsc* 200:83–104

Kripke ML, Munn CG, Jeevan A *et al.* (1990) Evidence that cutaneous antien presenting cells migrate to regional lymph nodes during contact sensitization. *J Immunol* 145:2833–8

Kubo A, Nagao K, Amagai M (2012) Epidermal barrier dysfunction and cutaneous sensitization in atopic diseases. *J Clin Invest* 122:440–7

Larson RP, Zimmerli SC, Comeau MR *et al.* (2010) Dibutyl phthalate-induced thymic stromal lymphopoietin is required for Th2 contact hypersensitivity responses. *J Immunol* 184:2974–84

Maruyama T, Iizuka H, Tobisawa Y *et al.* (2007) Influence of local treatments with capsaicin or allyl isothiocyanate in the sensitisation phase of a fluorescein-isothiocyanate-induced contact sensitivity model. *Int Arch Allergy Immunol* 143:144–54

Matsuki M, Yamashita F, Ishida-Yamamoto A *et al.* (1998) Defective stratum corneum and early neonatal death in mice lacking the gene for transglutaminase 1 (keratinocyte transglutaminase). *Proc Natl Acad Sci USA* 95:1044–9

Nakatsuji T, Kao MC, Fang JY *et al.* (2009) Antimicrobial property of lauric acid against *Propionibacterium acnes*: its therapeutic potential for inflammatory acne vulgaris. *J Invest Dermatol* 129:2480–8

Pisano JJ, Finlayson JS, Peyton MP (1968) Cross-link in fibrin polymerized by factor 13: epsilon-(gamma-glutamyl) lysine. *Science* 160:892–3

Russell LJ, DiGiovanna JJ, Rogers GR *et al.* (1995) Bale mutations in the gene for transglutaminase 1 in autosomal recessive lamellar ichthyosis. *Nat Genet* 9:279–83

Sandilands A, Smith FJ, Irvine AD *et al.* (2007) Filaggrin's fuller figure: A Glimpse into the Genetic Architecture of Atopic Dermatitis. *J Invest Dermatol* 127:1282–4

Scharschmidt TC, Man M-Q, Hatano Y *et al.* (2009) Filaggrin deficiency confers a paracellular barrier abnormality that reduces inflammatory thresholds to irritants and haptens. *J Allergy Clin Immunol* 124:496–506

Sardy M, Karpati S, Merkl B *et al.* (2002) Epidermal transglutaminase (Tase 3) is the autoantigen of dermatitis herpetiformis. *J Exp Med* 195:747–57

Sato K, Imai Y, Irimura T (1998) Contribution of dermal macrophage trafficking in the sensitisation phase of contact hypersensitivity. *J Immunol* 161:6835–44

Takeshita K, Yamasaki T, Akira S *et al.* (2004) Essential role of MHC II-independent CD4+ T cells, IL-4 and STAT6 in contact hypersensitivity induced by fluorescein isothiocyanate in the mouse. *Int Immunol* 16: 685–95